Journal of Physics A: Mathematical and Theoretical

PAPER • OPEN ACCESS

Multi-Hamiltonian structure of the epidemics model accounting for vaccinations and a suitable test for the accuracy of its numerical solvers

To cite this article: F Haas *et al* 2022 *J. Phys. A: Math. Theor.* **55** 225206

OPEN ACCESS
IOP Publishing

Journal of Physics A: Mathematical and Theoretical

J. Phys. A: Math. Theor. **55** (2022) 225206 (16pp)

https://doi.org/10.1088/1751-8121/ac6995

Multi-Hamiltonian structure of the epidemics model accounting for vaccinations and a suitable test for the accuracy of its numerical solvers

F Haas[1,*], **M Kröger**[2,*] **and R Schlickeiser**[3,4,*]

[1] Instituto de Física, Universidade Federal do Rio Grande do Sul, Av. Bento Gonçalves 9500, 91501-970 Porto Alegre, RS, Brazil
[2] Polymer Physics, Department of Materials, ETH Zurich, Zurich CH-8093, Switzerland
[3] Institut für Theoretische Physik, Lehrstuhl IV: Weltraum- und Astrophysik, Ruhr-Universität Bochum, D-44780 Bochum, Germany
[4] Institut für Theoretische Physik und Astrophysik, Christian-Albrechts-Universität zu Kiel, Leibnizstr. 15, D-24118 Kiel, Germany

E-mail: fernando.haas@ufrgs.br, mk@mat.etz.ch and rsch@tp4.rub.de

Received 16 November 2021, revised 24 March 2022
Accepted for publication 22 April 2022
Published 16 May 2022

Abstract

We derive a generalized Hamiltonian formalism for a modified susceptible–infectious–recovered/removed (SIR) epidemic model taking into account the population V of vaccinated persons. The resulting SIRV model is shown to admit three possible functionally independent Hamiltonians and hence three associated Poisson structures. The reduced case of vanishing vaccinated sector shows a complete correspondence with the known Poisson structures of the SIR model. The SIRV model is shown to be expressible as an almost Nambu system, except for a scale factor function breaking the divergenceless property. In the autonomous case with time-independent stationary ratios k and b, the SIRV model is shown to be a maximally super-integrable system. For this case we test the accuracy of numerical schemes that are suited to solve the stiff set of SIRV differential equations.

*Authors to whom any correspondence should be addressed.

Keywords: corona virus, Poisson structure, super-integrable system, epidemics, Nambu mechanics, Covid-19

(Some figures may appear in colour only in the online journal)

1. Introduction

Since their original development by Kermack and McKendrick [1] and refinement by Kendall [2] compartment models of epidemics have been widely used (for reviews see Hethcode [3], Keeling and Rohani [4], Estrada [5]) as they describe successfully the temporal evolution of epidemic outbreaks and also allow well-founded predictions on the hospitalization and death rates of such outbreaks (for a recent application to the Covid-19 virus see Kröger and Schlickeiser [6]). The simplest compartment model is the susceptible–infectious–recovered (SIR) model where persons from a considered population are assigned to the three compartments S (susceptible), I (infectious) and R (recovered/removed). The infection and recovery rates then regulate the transition probability between the compartments. Later refinements of the SIR-model such as the SEIR [7, 8], SIRD [9] and SIRS [10–12] have introduced additional compartments.

Recently, two of us [13] extended the standard SIR epidemic model by introducing a fourth compartment V of vaccinated persons and the vaccination rate $v(t)$ that regulates the relation between susceptible and vaccinated persons. The vaccination rate $v(t)$ competes with the infection ($a(t)$) and recovery ($\mu(t)$) rates in determining the time evolution of epidemics. Exact analytical inverse solutions $t(Q)$ for all relevant quantities $Q \in [S, I, R, V]$ of the resulting SIRV-model in terms of Lambert functions were derived for the semi-time case with time-independent ratios $k = \mu(t)/a(t)$ and $b = v(t)/a(t)$ between the recovery and vaccination rates to the infection rate, respectively. These inverse solutions can be approximated with high accuracy yielding the explicit time-dependence $Q(t)$ by inverting the Lambert functions. It was demonstrated that the values of the two ratios k and b as well as the initial fraction of infected persons $\eta \leqslant 1$ completely determine the reduced time evolution the SIRV-quantities $Q(\tau)$, where the reduced time defined by $\tau = \int_0^t \mathrm{d}t'\, a(t')$ accounts for any given time-dependence of the infection rate.

The existence of a generalized Hamiltonian formalism, also called Poisson structure, is an important property of dynamical systems. For instance, it allows the nonlinear stability analysis of stationary solutions in terms of the energy-Casimir method [14]. Three-dimensional Poisson structures have attracted some attention, being the lower dimensional case where a Hamiltonian description is not symplectic [15–21]. Historically the Poisson structure comes in an attempt to generalize canonical Hamiltonian mechanics while preserving its essential geometric properties.

In the case of the SIRV model, it is a four-dimensional (4D) dynamical system. Related to the SIRV model, the Hamiltonian structure of compartmental epidemiological models has been discussed [22]. However, the analysis presented here is more general as it holds for arbitrary time-dependent infection rates whereas the earlier study [22] is restricted to constant stationary infection rates. This generalization is important because non-pharmaceutical interventions generate time-varying infection rates during an pandemic outbreak. The study of 4D Poisson structures from a general point of view was done in references [23, 24] and for Ermakov systems in reference [25]. Five [26], six [27–29] or generic N-dimensional Poisson structures have been also discussed [30–34].

This work is organized as follows. In section 2 the SIRV equations and the basic properties of generalized Hamiltonian systems are reviewed. The three possible Hamiltonians for the SIRC model are derived, together with the analysis of the reduced, SIR model limit without a vaccinated population. Section 3 considers the stationary case where the system is not explicitly time-dependent. Here we investigate the applicability of numerical solvers. Section 4 shows some properties of the third Hamiltonian of the SIRV system, which appears in an integral form not expressible in terms of elementary functions. Section 5 discusses the multi-Hamiltonian structure of the SIRV model and section 5.4 shows the lower-dimensional SIR reduction of these structures dropping the vaccinated population. Section 6 is reserved to the conclusions.

2. Multi-Hamiltonian structure of the SIRV model

We start with the dynamical SIRV equations [13] modeling the fraction of susceptible (S), infected (I), recovered/removed (R), and vaccinated (V) population in the course of time t,

$$\frac{\mathrm{d}S}{\mathrm{d}t} = -a\,S\,I - v\,S, \qquad \frac{\mathrm{d}I}{\mathrm{d}t} = a\,S\,I - \mu\,I,$$
$$\frac{\mathrm{d}R}{\mathrm{d}t} = \mu\,I, \qquad \frac{\mathrm{d}V}{\mathrm{d}t} = v\,S, \tag{1}$$

where $a = a(t)$, $\mu = \mu(t)$, and $v = v(t)$ are time-dependent transition rates. The SIRV model distinguishes between vaccinated and non-vaccinated individuals. The vaccinated individuals are assumed to be completely immune to the virus and proceed with rate $v(t)$ to the compartment of recovered individuals. In contrast, the non-vaccinated individuals can get infected with the rate $a(t)$, and thus contribute to the fraction of new infections $\dot{J}(t) = a(t)S(t)I(t)$ that determine the hospitalization and death rates. In the absence of vaccination, $v = 0$, and the SIRV model reduces to the SIR model introduced a century ago [1, 2]. Although not strictly necessary, it is convenient to eliminate one of the time-dependent parameters in equation (2) using the reduced time

$$\tau = \int_0^t \mathrm{d}t'\, a(t'), \tag{2}$$

so that

$$\frac{\mathrm{d}S}{\mathrm{d}\tau} = -\,S\,I - b\,S, \qquad \frac{\mathrm{d}I}{\mathrm{d}\tau} = \,S\,I - k\,I,$$
$$\frac{\mathrm{d}R}{\mathrm{d}\tau} = k\,I, \qquad \frac{\mathrm{d}V}{\mathrm{d}\tau} = b\,S, \tag{3}$$

where $k = k(\tau) = \mu/a$ and $b = b(\tau) = v/a$. We emphasize that in the following we allow the ratios $k(\tau)$ and $b(\tau)$ to be time-dependent.

2.1. Generalized Hamiltonian formalism

In a generalized Hamiltonian formulation [18, 22] the dynamical system is written as

$$\frac{\mathrm{d}x^i}{\mathrm{d}\tau} = \{x^i, H\} = J^{ij}\partial_j H, \tag{4}$$

where $H = H(x^i, \tau)$ is the Hamiltonian function and the Poisson bracket $\{,\}$ is defined by

$$\{A, B\} = \partial_i A \, J^{ij} \, \partial_j B, \tag{5}$$

where A, B are generic functions and the structure functions $J^{ij} = -J^{ji}$ are the components of an antisymmetric two-tensor. Summation convention is being employed, and $\partial_i = \partial/\partial x^i$.

In order to ensure the Jacobi identity $\{A, \{B, C\}\} + \{B, \{C, A\}\} + \{C, \{A, B\}\} = 0$, the equation

$$J^{ij}\partial_i J^{kl} + J^{ik}\partial_i J^{lj} + J^{il}\partial_i J^{jk} = 0, \tag{6}$$

must be satisfied.

For a 4D dynamical system with $x^i = (x^1, x^2, x^3, x^4)$, equation (6) amounts to

$$J^{i1}\partial_i J^{23} + J^{i2}\partial_i J^{31} + J^{i3}\partial_i J^{12} = 0, \tag{7}$$

$$J^{i1}\partial_i J^{24} + J^{i2}\partial_i J^{41} + J^{i4}\partial_i J^{12} = 0, \tag{8}$$

$$J^{i1}\partial_i J^{34} + J^{i3}\partial_i J^{41} + J^{i4}\partial_i J^{13} = 0, \tag{9}$$

$$J^{i2}\partial_i J^{34} + J^{i3}\partial_i J^{42} + J^{i4}\partial_i J^{23} = 0. \tag{10}$$

Moreover, the Hamiltonian must satisfy

$$\frac{\mathrm{d}x^i}{\mathrm{d}\tau} \, \partial_i H = \partial_i H \, J^{ij} \, \partial_j H = \{H, H\} = 0. \tag{11}$$

Therefore

$$\frac{\mathrm{d}H}{\mathrm{d}\tau} = \frac{\partial H}{\partial \tau}, \tag{12}$$

so that if H is not explicitly time-dependent it is a constant of motion (or first integral).

2.2. Three Hamiltonians for the SIRV model

For the SIRV model, it is useful to define $(S, I, R, V) = (x^1, x^2, x^3, x^4) = (x, y, z, w)$, so that equation (3) read

$$\frac{\mathrm{d}x}{\mathrm{d}\tau} = -\,x\,y - b\,x, \quad \frac{\mathrm{d}y}{\mathrm{d}\tau} = x\,y - k\,y,$$
$$\frac{\mathrm{d}z}{\mathrm{d}\tau} = k\,y, \qquad \frac{\mathrm{d}w}{\mathrm{d}\tau} = b\,x. \tag{13}$$

According to equation (11) a Hamiltonian for the SIRV model then solves the partial differential equation

$$-(xy + bx)\frac{\partial H}{\partial x} + (xy - ky)\frac{\partial H}{\partial y} + ky\frac{\partial H}{\partial z} + bx\frac{\partial H}{\partial w} = 0. \tag{14}$$

Using the method of characteristics, equation (14) is equivalent to the Pfaff system

$$-\frac{\mathrm{d}x}{xy + bx} = \frac{\mathrm{d}y}{xy - ky} = \frac{\mathrm{d}z}{ky} = \frac{\mathrm{d}w}{bx}, \tag{15}$$

so that H is a constant on characteristics. It is possible to solve equation (14) for three independent functions. One of them, which we call $H = H_1$, is a distinguished first integral of the SIRV equations, namely

$$H_1 = H_1(x, y, z, w) = x + y + z + w. \tag{16}$$

As H_1 does not explicitly depend on time τ, it is a constant of motion which reflects the well-known sum constraint requirement [35] if combined with the semi-time initial conditions [13] $x(0) = 1 - \eta$, $y(0) = \eta$ and $z(0) = w(0) = 0$.

A second function which can play the role of Hamiltonian is

$$\begin{aligned} H_2 = H_2(x, y) &= x - k \ln x + y + b \ln y \\ &= S + I - k(\tau) \ln S + b(\tau) \ln I, \end{aligned} \tag{17}$$

as can be verified by *a posteriori* resubstitution. In the general case of time-dependent ratios $k(\tau)$ and $b(\tau)$ the function H_2 is not a constant of motion; only in the case of stationary values of these ratios H_2 is a first integral of motion.

2.3. Third Hamiltonian

The derivation of the third Hamiltonian function is more involved. We consider the third characteristic equation (15) reading

$$\mathrm{d}z = -\frac{k\,y\,\mathrm{d}x}{x\,y + b\,x}, \tag{18}$$

and express y in terms of x along characteristics by inverting equation (17) written as

$$y + b \ln y = H_2 - x + k \ln x. \tag{19}$$

With $y = e^{-Y}$ equation (19) becomes

$$e^{-Y} = b\left(Y + \frac{H_2 - x}{b} + \frac{k}{b} \ln x\right), \tag{20}$$

with the solution

$$Y = \frac{x - H_2 - k \ln x}{b} + W[\xi(x)] = -\ln(b\xi) + W(\xi), \tag{21}$$

in terms of the Lambert function defined by [36, 37]

$$W(\xi)e^{W(\xi)} = \xi, \tag{22}$$

and

$$\xi = \xi(x) = \frac{x^{k/b} \exp\left(\frac{H_2 - x}{b}\right)}{b}. \tag{23}$$

Consequently we obtain for the solution of equation (19)

$$y = e^{-Y} = b\xi e^{-W(\xi)} = bW(\xi), \tag{24}$$

where we used equation (22) in the last step. Inserting equation (24) then provides for equation (18)

$$\frac{\mathrm{d}z}{\mathrm{d}x} = -\frac{kW[\xi(x)]}{x\{1 + W[\xi(x)]\}} = -\frac{k\xi(x)}{x}\frac{\mathrm{d}W}{\mathrm{d}\xi}, \tag{25}$$

where we made use of Lambert's differential equation

$$\frac{\mathrm{d}W}{\mathrm{d}\xi} = \frac{W(\xi)}{\xi[1+W(\xi)]}. \tag{26}$$

At this stage W can be either the principal Lambert function ($W_0 \geqslant -1$) or the second branch ($W_{-1} \leqslant -1$). The Lambert functions $W(\xi)$ are real valued for $\xi \geqslant -1/e \approx -0.37$ which presently is always satisfied since $x \geqslant 0, b > 0$.

Integrating equation (25) yields

$$\begin{aligned}\tilde{H} &= z + k\int^x \frac{\mathrm{d}x\xi}{x}\frac{\mathrm{d}W}{\mathrm{d}\xi} = z + k\int^x \frac{\mathrm{d}x\xi}{x\frac{\mathrm{d}\xi}{\mathrm{d}x}}\frac{\mathrm{d}W}{\mathrm{d}x} \\ &= z + k\int^x \frac{\mathrm{d}x}{x\frac{\mathrm{d}\,\ln\,\xi}{\mathrm{d}x}}\frac{\mathrm{d}W}{\mathrm{d}x}.\end{aligned} \tag{27}$$

With

$$\ln\,\xi = \frac{k}{b}\,\ln\,x - \ln\,b + \frac{H_2 - x}{b}, \tag{28}$$

we obtain

$$x\frac{\mathrm{d}\,\ln\,\xi}{\mathrm{d}x} = \frac{k-x}{b}, \tag{29}$$

along characteristics, that is, with H_2 constant. With equation (29) inserted equation (27) yields

$$\tilde{H} = z + kb\int^x \frac{\mathrm{d}x}{k-x}\frac{\mathrm{d}W}{\mathrm{d}x}, \tag{30}$$

as a possible Hamiltonian. While the form (30) is quite acceptable, it is more convenient to consider

$$\begin{aligned}H_3 &= H_1 - H_2 - \tilde{H} \\ &= w + k\,\ln\,x - b\,\ln\,y - bk\int^x \frac{\mathrm{d}x}{k-x}\frac{\mathrm{d}W}{\mathrm{d}x},\end{aligned} \tag{31}$$

to have a more clear reduction to the SIR case. We emphasize that in the treatment of equation (31) one has $W = W(\xi(x))$ where $\xi(x)$ is given by equation (23), parametrically dependent on H_2, but after integration one replaces H_2 therein by its expression (17). Using equations (26) and (29) we also have

$$\begin{aligned}H_3 &= w + k\,\ln\,x - b\,\ln\,y - k\int^x \frac{\mathrm{d}x}{x}\frac{W(\xi)}{1+W(\xi)} \\ &= w + k\,\ln\,x - b\,\ln\,y - k\int^x \frac{\mathrm{d}q}{q}\frac{Q(x,y,q)}{1+Q(x,y,q)},\end{aligned} \tag{32}$$

where

$$Q(x,y,q) = W(\xi) = W\left[\frac{y}{b}\left(\frac{q}{x}\right)^{k/b}\,\exp\left(\frac{x+y-q}{b}\right)\right]. \tag{33}$$

We emphasize that the existence of this third Hamiltonian (31) has been missed in the earlier analysis of reference [22].

2.4. Limiting SIR-case

The SIR model [1] is a 3D dynamical system with $(x^1, x^2, x^3) = (x, y, z) = (S, I, R)$ obtained from equation (13) in the absence of vaccination, i.e., upon setting $w = 0$, $b = 0$,

$$\frac{\mathrm{d}x}{\mathrm{d}\tau} = -\,x\,y, \qquad \frac{\mathrm{d}y}{\mathrm{d}\tau} = \,x\,y - k\,y, \qquad \frac{\mathrm{d}z}{\mathrm{d}\tau} = k\,y. \tag{34}$$

Its generalized Hamiltonian formulation was analyzed some time ago [18–21], also possessing a multi-Hamiltonian structure, in this case a bi-Hamiltonian structure, becoming maximally super-integrable in the autonomous case. We can select the possible Hamiltonians $H_1 = x + y + z$, which is the reduced version ($w = 0$) of the universal constant of motion for the SIRV model, and $H_2 = x - k \ln x + y$, which is the reduced version of H_2 given by equation (17) for $b = 0$. In this singular limit situation equation (18) reads

$$\frac{\mathrm{d}z}{\mathrm{d}x} + \frac{k}{x} = 0, \tag{35}$$

yielding upon integration

$$\tilde{H} = z + k\,\ln\,x = H_1 - H_2 \neq 0, \tag{36}$$

when $w = 0, b = 0$ instead of equation (30) with the Lambert function, so that correctly

$$H_3^{\mathrm{SIR}} = H_1 - H_2 - \tilde{H} = 0, \tag{37}$$

in the SIR limit. Any choice, different from equation (37), would give a SIR reduction with a third non-zero Hamiltonian function being functionally dependent on the remaining $H_{1,2}$.

3. Stationary ratios *k* and *b*

In the case when k, b are time-independent, which was treated in detail in reference [13], we have $H_{2,3}$ from equations (17) and (32) as additional constants of motion reading

$$\begin{aligned} H_2 &= 1 - k\,\ln(1-\eta) + b\,\ln\,\eta, \\ H_3 &= k\,\ln(1-\eta) - b\,\ln\,\eta - k\int^{1-\eta} \frac{\mathrm{d}q}{q}\,\frac{Q(1-\eta,\eta,q)}{1+Q(1-\eta,\eta,q)}, \end{aligned} \tag{38}$$

using again the initial conditions of the semi-time SIRV-model [13] $x(0) = 1 - \eta$, $y(0) = \eta$ and $z(0) = w(0) = 0$.

3.1. Time asymptotics

As argued in reference [13], with $b > 0$ and assuming z residing in the finite interval [0, 1], one has $x_\infty = x(\tau = \infty) = 0$. The existence of three constants of motion allows some precise predictions for the time asymptotics as $\tau \to \infty$. For definiteness, suppose $x_\infty = 0$. To keep H_2 constant, then it is necessary that $y_\infty = y(\tau = \infty) = 0$ too, but according to

$$y_\infty = A\,x_\infty^{k/b}, \quad A = \frac{e^{1/b}\,\eta}{(1-\eta)^{k/b}}. \tag{39}$$

In this context, to keep a constant H_1 one then needs $z_\infty + w_\infty = 1$, where $z_\infty = z(\tau = \infty)$ and $w_\infty = w(\tau = \infty)$. Actually it is possible to manage H_3 in this limit, to derive

$$z_\infty = k \int^{q=1-\eta} \frac{\mathrm{d}q}{q} \frac{Q(1-\eta,\eta,q)}{1+Q(1-\eta,\eta,q)} - k \int^{q=0} \frac{\mathrm{d}q}{q} \frac{Q_\infty(q)}{1+Q_\infty(q)}, \tag{40}$$

where

$$\begin{aligned} Q_\infty(q) &= W\left[\frac{y_\infty}{b}\left(\frac{q}{x_\infty}\right)^{k/b} \exp\left(\frac{x_\infty + y_\infty - q}{b}\right)\right] \\ &= W\left[\frac{\eta \exp[(1-q)/b] q^{k/b}}{b(1-\eta)^{k/b}}\right]. \end{aligned} \tag{41}$$

Finally, one has $w_\infty = 1 - z_\infty$.

3.2. SIR-case

In the limiting SIR-case with $b = 0$ clearly

$$H_2 = x + y - k \ln x = S + I - k \ln S, \tag{42}$$

is the only constant of motion besides the sum constraint $H_1 = 1$. As demonstrated before [6, 13] for stationary ratio k the exact analytical solution of the SIR-model as a function of the reduced time (2) is given by

$$\begin{aligned} x(\tau) &= S(\tau) = 1 - J(\tau), \\ y(\tau) &= I(\tau) = 1 + k\epsilon - x(\tau) + k \ln x(\tau), \\ z(\tau) &= R(\tau) = -k[\epsilon + \ln x(\tau)], \end{aligned} \tag{43}$$

in terms of the cumulative fraction of new cases $J(\tau)$ obeying the integral

$$\tau = \int_\eta^J \frac{\mathrm{d}\psi}{(1-\psi)[\psi + k\epsilon + k \ln(1-\psi)]}, \tag{44}$$

with $\eta = 1 - e^{-\epsilon}$ and the initial condition $I(0) = \eta$. By direct insertion it is straightforward to prove that the solution (43) indeed obeys the constant of motion (42).

3.3. Application: accuracy of numerical solvers

In practice, the SIR and SIRV model equations with time-independent ratios k and b are commonly solved numerically, while some analytic approximants exist. However, the SIRV equations constitute a stiff differential set of equations, for which certain numerical methods for solving the equation are numerically instable.

Having explored the Hamiltonian structure we can restrict ourselves to the autonomous case to test the accuracy of numerical solvers. The ideal solver should keep all the Hamiltonians unchanged during the course of time. To make sure our results are reproducable, and the underlying methods well documented, we subjected a large number of methods offered by the commercial software packages Mathematica™ and Matlab™ to our test [38, 39]. Because

Table 1. For a large number of methods available in Mathematica™ 12[38] and Matlab™ R2019a [39] we here provide representative results for the decadic logarithm of the mismatch $\Delta H_j = |H_j(t=100) - H_j(t=0)|$ for $j \in \{2,3\}$ using SIRV parameters $k = b = 0.5$, $\eta = 0.1$. For all Mathematica™ routines we used the specified working precision (WorkingPrecision equal to PrecisionGoal). Remaining methods available in Matlab™ for non-stiff differential equations do not produce any result.

$\log_{10}\Delta H_2$	$\log_{10}\Delta H_3$	Precision	Software	Name of method
−7.6304	−7.8309	20	Mathematica™ 12	Adams, MaxDifferenceOrder → 10
−6.2650	−6.4622	20	Mathematica™ 12	BDF
−5.9661	−6.1608	20	Mathematica™ 12	Adams, MaxDifferenceOrder → 2
−4.5892	−4.7877	10	Mathematica™ 12	ExplicitModifiedMidpoint
−3.9041	−4.1018	10	Mathematica™ 12	LinearlyImplicitMidpoint
−3.8239	−3.9838	10	Mathematica™ 12	Adams, MaxDifferenceOrder → 10
−3.3633	−3.5612	10	Mathematica™ 12	ExplicitMidpoint
−2.9477	−3.1377	10	Mathematica™ 12	Adams, MaxDifferenceOrder → 2
−2.9253	−2.9941	10	Mathematica™ 12	LinearlyImplicitModifiedMidpoint
−1.9612	−2.1605	10	Mathematica™ 12	ExplicitRungeKutta, DifferenceOrder → 2
−0.5624	−0.7999	10	Mathematica™ 12	ImplicitRungeKutta, DifferenceOrder → 2
−0.2633	−0.3985	10	Mathematica™ 12	BDF
−0.0351	−0.3670	20	Mathematica™ 12	ImplicitRungeKutta, DifferenceOrder → 10
−0.1636	−0.3314	—	Matlab™ R2019a	ode15s
0.1166	−0.0815	—	Matlab™ R2019a	ode23t
0.1539	−0.1066	—	Matlab™ R2019a	ode23tb
0.1969	0.9437	10	Mathematica™ 12	ImplicitRungeKutta, DifferenceOrder → 10
1.7008	1.6548	10	Mathematica™ 12	ExplicitRungeKutta, DifferenceOrder → 10
1.7008	1.6548	10	Mathematica™ 12	IDA, ImplicitSolver → FixedPoint
1.7008	1.6548	20	Mathematica™ 12	ExplicitRungeKutta, DifferenceOrder → 10
2.8889	0.6104	10	Mathematica™ 12	ExplicitEuler, variable step size
2.8976	−0.0007	10	Mathematica™ 12	LinearlyImplicitEuler
3.0376	3.0720	20	Mathematica™ 12	LinearlyImplicitMidpoint
3.0605	3.0968	20	Mathematica™ 12	ImplicitRungeKutta, DifferenceOrder → 2
4.4480	4.5197	20	Mathematica™ 12	ExplicitModifiedMidpoint
4.7576	4.8286	20	Mathematica™ 12	ExplicitMidpoint
4.7628	4.8323	20	Mathematica™ 12	ExplicitRungeKutta, DifferenceOrder → 2
9.4727	9.5026	20	Mathematica™ 12	LinearlyImplicitModifiedMidpoint
9.5362	1.1878	—	Mathematica™ 12	ExplicitEuler, fixed step size 0.01
9.5355	7.0437	—	Mathematica™ 12	ExplicitEuler, fixed step size 0.001
10.2583	10.2906	20	Mathematica™ 12	ExplicitEuler, variable step size
10.2583	10.2906	20	Mathematica™ 12	LinearlyImplicitEuler

results are seen to not depend qualitatively on the choice of initial conditions, we have performed benchmark tests at the classical semi-time SIR initial conditions mentioned earlier: $x(0) = 1 - \eta$, $y(0) = \eta$, using $\eta = 0.1$, while $z(0) = w(0) = 0$. As both ratios k, b are semi-positive and usually residing on the interval [0, 1], we have used $k = b = 0.5$ for the tests to be reported here. With these choices, the initial values for Hamiltonians are $H_1(0) = 1$, $H_2(0) = 1 - \ln(3) \approx -0.0986$, and $H_3(0) \approx 0.8516$ according to equation (32) with equation (33).

For each of the methods collected in table 1 we then measured the absolute deviations $\Delta H_j(t) = |H_j(t) - H_j(0)|$ for $j \in \{1, 2, 3\}$ as function of time, up to $t = 100$. Actually, we

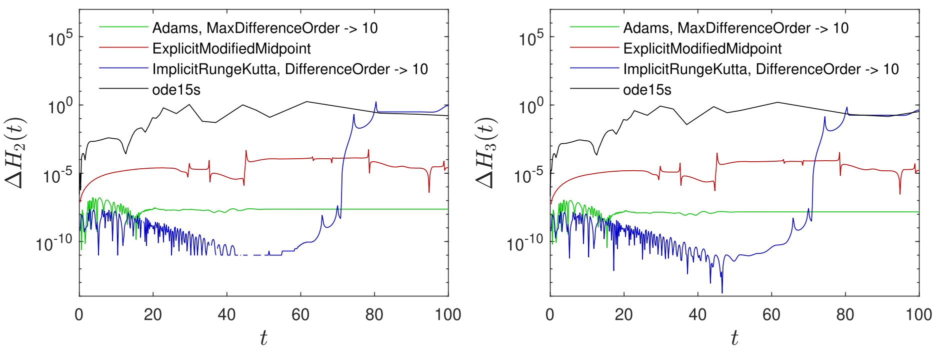

Figure 1. Time evolution of the mismatch $\Delta H_2(t) = |H_2(t) - H_2(0)|$ and $\Delta H_3(t) = H_3(t) - H_3(0)$ for selected numerical solvers, cf, table 1. The predictor–corrector Adams solver implemented in Mathematica$^{\mathrm{TM}}$ turned out to best keep both Hamiltonians at their initial values of order unity.

tested many more settings (order 10^5), as several of the methods have additional parameters than can be varied to tune the algorithm. In this sense, table 1 contains representative, and to our opinion, the most relevant results. It offers an assessment of both explicit and indirect methods, methods for stiff and non-stiff ordinary differential equations, methods with constant and adaptive time steps, predictor- and corrector steps, and results for different choices of the numerical precision employed.

Selected time series are shown in figure 1. As the deviations tend to be most pronounced at the end of the time interval, we collect in table 1 only the final values $\Delta H_j(100)$ for all the algorithms. We do not include the values for ΔH_1, because all methods succeed in keeping the sum constraint $H_1(t) = 1$ intact to very high precision.

We find the 10th order predictor–corrector Adams method works perfectly fine. Adam's method is a numerical method for solving first-order ordinary differential equations of the SIRV form $\mathrm{d}x/\mathrm{d}t = f(x, t)$, that combines the explicit Adams–Bashforth and implicit Adams–Moulton steps. Let $\Delta t = t_{n+1} - t_n$ be the step interval, and consider the Maclaurin series of x about t_n, $x_{n+1} = x_n + (\mathrm{d}x/\mathrm{d}t)_n(t - t_n) + (1/2)(\mathrm{d}^2x/\mathrm{d}t^2)_n(t - t_n)^2 + \mathcal{O}(t - t_n)^3$ and $(\mathrm{d}x/\mathrm{d}t)_{n+1} = (\mathrm{d}x/\mathrm{d}t)_n + (\mathrm{d}^2x/\mathrm{d}t^2)_n(t - t_n)^2 + \mathcal{O}(t - t_n)^3$. Here, the derivatives of x are given by the backwards differences [38]. For first-order interpolation, the method proceeds by iterating the expression $x_{n+1} = x_n + f(x_n, t_n)\Delta t$. The method is extended to arbitrary order using the finite difference integration formula from Beyer [40]. On the other end, the explicit or implicit Euler methods should not be used, such as $x_{n+1} = x_n + f(x_n, t_n)\Delta t$ or $x_{n+1} = x_n + f(x_{n+1}, t_n)\Delta t$, respectively. It is also worthwhile noticing that all methods available in Matlab$^{\mathrm{TM}}$ do not perform very well. Table 1 mentions three out of the seven Matlab methods that produce a numerical (as opposed to not-a-number) result up to $t = 100$ for our benchmark case. The ones that work are all designed for stiff (ode15s) or moderately stiff (ode23t, ode23tb) ordinary differential equations.

4. Analytic properties of the third Hamiltonian (32)

It is not very commonplace to have a constant of motion in terms of a definite integral as is the case of H_3 in equation (32). Hence it is convenient to provide a recipe for partial derivatives of such class of functions. We note

$$\frac{\partial}{\partial x}\int \mathrm{d}x\, f(x,c) = \frac{\partial}{\partial x}\int^{x}\mathrm{d}x'\, f(x',c(x,y)) = f(x,c(x,y)) + \frac{\partial c}{\partial x}\int^{x}\mathrm{d}x\,\frac{\partial f}{\partial c}, \tag{45}$$

$$\frac{\partial}{\partial y}\int \mathrm{d}x\, f(x,c) = \frac{\partial}{\partial y}\int^{x}\mathrm{d}x'\, f(x',c(x,y)) = \frac{\partial c}{\partial y}\int^{x}\mathrm{d}x\,\frac{\partial f}{\partial c}, \tag{46}$$

where $f(x,c)$ and $c = c(x,y)$ are arbitrary functions of the indicated arguments. One then finds

$$\frac{\partial H_3}{\partial x} = \frac{kb}{x(y+b)} - \frac{k}{b}\left(1-\frac{k}{x}\right)\int^{x}\frac{\mathrm{d}x\,W(\xi)}{x[1+W(\xi)]^3}, \tag{47}$$

$$\frac{\partial H_3}{\partial y} = -\frac{b}{y} - \frac{k}{b}\left(1+\frac{b}{y}\right)\int^{x}\frac{\mathrm{d}x\,W(\xi)}{x[1+W(\xi)]^3}, \tag{48}$$

which together with $\partial H_3/\partial z = 0$, $\partial H_3/\partial w = 1$ shows that $H = H_3$ indeed solves equation (14). For the derivation of equations (47) and (48), one starts from H_3 in equation (32) applying the identities in equation (45) with

$$f(x,c) = \frac{1}{x}\frac{W(\xi)}{1+W(\xi)}, \qquad c = H_2(x,y), \tag{49}$$

with $\xi = \xi(x)$ from equation (23), parametrically dependent on H_2. A final step uses $W(\xi) = y/b$ according to equation (24).

5. Poisson structures

The existence of three possible Hamiltonians allows us to write

$$\frac{\mathrm{d}x^i}{\mathrm{d}\tau} = A\,\varepsilon^{ijkl}\,\partial_j H_1\,\partial_k H_2\,\partial_l H_3, \tag{50}$$

where ε^{ijkl} is the 4D Levi-Civita symbol, which equals 1 for even permutations of $\{1,2,3,4\}$, -1 for odd permutations and zero otherwise, and where $A = A(x,y,z,w,t)$ is a scale factor to be determined. The form (50) shows that equation (11) is immediately satisfied, due to the anti-symmetry of ε^{ijkl}. In the case of the SIRV model, a direct calculation yields

$$A = x\,y. \tag{51}$$

It can be observed that a dynamical system in the form (50) is almost a Nambu system [41], which in the 4D case is given by

$$\frac{\mathrm{d}x^i}{\mathrm{d}\tau} = \frac{\partial\{x^i,H_1,H_2,H_3\}}{\partial\{x,y,z,w\}}, \tag{52}$$

where $\partial\{x^i,H_1,H_2,H_3\}/\partial\{x,y,z,w\}$ denotes the four-dimensional Jacobian matrix. Nambu mechanics is known as a possible generalization of Hamiltonian mechanics preserving the divergenceless property, see [42] for a recent review. The SIRV model is not exactly a Nambu system since it is not divergenceless, which reflects in the scale factor $A \neq 1$ in equation (51). Nevertheless one has

$$\frac{\partial}{\partial x^i}\left(\frac{1}{A}\frac{\mathrm{d}x^i}{\mathrm{d}\tau}\right) = 0. \tag{53}$$

In this context the scale function A is also termed inverse Jacobi multiplier [17]. Alternatively, the case with a scale factor $A \neq 1$ is also known as non-canonical Nambu system, which has applications in the motion of three point vortices in the plane [43]. With a dynamical rescaling of time $\tau \to \tau'$ where $\mathrm{d}\tau' = A\mathrm{d}\tau$, then the SIRV model can be cast in the form (52) (with τ replaced by τ') which becomes divergenceless. This could—formally at least—allow building a local canonical symplectic structure thanks to Darboux's theorem [17].

In equation (50) there is no special role of any of the functions $H_{1,2,3}$, all of them with the status of a Hamiltonian, in spite of the pivotal character of H_1 which is always a first integral and which is known to be conserved from the very beginning. Therefore one has a multi-Hamiltonian structure with an associated generalized Poisson bracket, as will be readily proven. In this regard, within a given Poisson structure, it is relevant to know its Casimir functions. A Casimir function C by definition is a function in involution with any other function on phase space. Therefore it satisfies

$$J^{ij}\partial_j C = 0. \tag{54}$$

We are now in a position to enumerate the Poisson structures of the SIRV model, as follows.

5.1. Poisson structure I

From comparison between equations (4) and (50) one can chose

$$H = H_1, \quad J^{ij} = A\,\varepsilon^{ijkl}\,\partial_k H_2\,\partial_l H_3, \quad A = xy. \tag{55}$$

It can be shown that such antisymmetric tensor always satisfies the Jacobi identities (7)–(10), for arbitrary differentiable functions A and $H_{2,3}$. Therefore one has an admissible Poisson structure with H_1 playing the role of Hamiltonian, while $H_{2,3}$ are readily seen to be Casimir functions, immediately satisfying equation (54). More explicitly, one has

$$\begin{aligned} &J^{12} = 0, \quad J^{23} = (x-k)y, \quad J^{31} = x(y+b) \\ &J^{14} = 0, \quad J^{24} = 0, \quad J^{34} = -bx, \end{aligned} \tag{56}$$

with the remaining components given by antisymmetry.

5.2. Poisson structure II

In the same spirit, one has the Poisson structure

$$H = H_2, \quad J^{ij} = xy\,\varepsilon^{ijkl}\,\partial_k H_3\,\partial_l H_1, \tag{57}$$

which also reproduces the equations of motion and satisfies the Jacobi identities. In this case $H_{1,3}$ are the Casimir functions. More explicitly, one has

$$
\begin{aligned}
J^{12} &= -xy, \\
J^{23} &= -xy + \frac{bky}{y+b} - \frac{k}{b}(x-k)y \int \frac{\mathrm{d}x}{x} \frac{W(\xi)}{[1+W(\xi)]^3}, \\
J^{31} &= -xy - bx - \frac{k}{b}x(y+b) \int \frac{\mathrm{d}x}{x} \frac{W(\xi)}{[1+W(\xi)]^3}, \\
J^{14} &= -bx - \frac{k}{b}x(y+b) \int \frac{\mathrm{d}x}{x} \frac{W(\xi)}{[1+W(\xi)]^3}, \\
J^{24} &= -\frac{bky}{y+b} + \frac{k}{b}(x-k)y \int \frac{\mathrm{d}x}{x} \frac{W(\xi)}{[1+W(\xi)]^3}, \\
J^{34} &= bx + \frac{bky}{y+b} + \frac{k}{b}(bx+ky) \int \frac{\mathrm{d}x}{x} \frac{W(\xi)}{[1+W(\xi)]^3},
\end{aligned}
\tag{58}
$$

which can be checked to satisfy the Jacobi identities.

5.3. Poisson structure III

Finally, one can chose $H = H_3$ as the Hamiltonian, in which case

$$
J^{ij} = xy\,\varepsilon^{ijkl}\,\partial_k H_1\,\partial_l H_2, \tag{59}
$$

with $H_{1,2}$ playing the role of Casimirs. More explicitly,

$$
\begin{aligned}
J^{12} &= 0, & J^{23} &= -(x-k)y, \\
J^{31} &= -x(y+b), & J^{14} &= -x(y+b), \\
J^{24} &= (x-k)y, & J^{34} &= bx + ky,
\end{aligned}
\tag{60}
$$

with the remaining structure functions following from the antisymmetry.

In passing we note that the autonomous situation has a formal solution thanks to the complete integrability, or super-integrability in this case. A n-dimensional dynamical system possessing $(n-1)$-first integrals is known as a maximally super-integrable system [44]. The SIRV model is therefore maximally super-integrable in the autonomous case. An exact solution can then be found as follows. One can at least formally select one of the dynamical variables (say, x) to express the remaining in terms of it. Namely, from equations (23) and (24) one has $y = y(x)$. In the continuation one has $w = w(x)$ from equations (31) or (32) and finally $z = z(x)$ from equation (16). The trajectories so obtained do not take into account the temporal dynamics, as done in earlier work [13].

5.4. Poisson structures for the limiting SIR-case

For the limiting SIR model we selected already the possible Hamiltonians $H_1 = x + y + z$, and $H_2 = x - k\ln x + y$. It is almost immediate to write

$$
\frac{\mathrm{d}\mathbf{x}}{\mathrm{d}\tau} = xy\nabla H_1 \times \nabla H_2, \quad \mathbf{x} = (x, y, z), \tag{61}
$$

or

$$
\frac{\mathrm{d}x^i}{\mathrm{d}\tau} = xy\varepsilon^{ijk}\,\partial_j H_1\,\partial_k H_2, \tag{62}
$$

where ε^{ijk} is the 3D Levi-Civita symbol. Therefore one has the two Poisson structures I and II, related to H_1 and H_2. As remarked before, the SIRV Poisson structure III collapses in the SIR limit, due to $H_3 = 0$ in this case.

(a) If the Hamiltonian is $H = H_1$, the Jacobian is given by

$$J^{ij} = xy\varepsilon^{ijk}\,\partial_k H_2, \tag{63}$$

with Casimir H_2. Explicitly,

$$J^{12} = 0, \qquad J^{23} = (x-k)y, \qquad J^{31} = xy. \tag{64}$$

This corresponds to the Poisson structure I of the SIRV model setting $b = 0$, together with $J^{i4} = 0$.

(b) If the Hamiltonian is $H = H_2$, one has

$$J^{ij} = -xy\,\varepsilon^{ijk}\,\partial_k H_1, \tag{65}$$

with Casimir H_1. Explicitly,

$$J^{12} = J^{23} = J^{31} = -xy. \tag{66}$$

This corresponds to the Poisson structure II of the SIRV model setting $b = 0$, together with $J^{i4} = 0$, and omitting the integrals with the Lambert function. These integrals do not play any role in the SIR limit, since the characteristic equation (18) with $b = 0$ does not involve the Lambert function, as remarked.

6. Conclusion

The partial differential equation (14) for the Hamiltonian function of the SIRV model is exactly solvable, yielding three possible functionally independent Hamiltonians. While two of them (H_1 and H_2) are expressible in terms of elementary function, the third one (H_3) involves an integral containing the Lambert function, a somewhat unusual circumstance. Our analysis of the Hamiltonian properties of the SIRV-model is more general than earlier work as it holds for arbitrary time dependent infection rates due to the introduction of the reduced time. Nevertheless, the result allows to express the SIRV model as a non-canonical Nambu system, directly associated to three Poisson structures. The corresponding structure functions J^{ij} defining the generalized Poisson bracket have been determined, and verified to be in accordance with the Jacobi identity. The Poisson structure class II also depends on integrals of the Lambert function, in spite of the Hamiltonian H_2 to be a simpler function of the dynamical variables. The corresponding Casimir functions commuting with all phase space functions have been determined for the three generalized Hamiltonian descriptions. The derivation of the third Hamiltonian H_3 shows the SIRV model to be completely integrable in the autonomous, or stationary case. The reduction to the lower-dimensional case where the vaccinated population is absent shows a complete correspondence between the extended Poisson structures I and II of SIRV model with the previously known Poisson structures of the SIR model, while the Poisson structure class III of SIRV collapses in this case, as it should. In a sense the Poisson structure I of the SIRV model is privileged since it is the only where both the Hamiltonian and the structure functions do not have integrals unevaluated in terms of elementary functions. However, one of its Casimir functions (namely H_3) involves an integral containing the Lambert function. As a side-result we find that Adam's predictor–corrector scheme appears most suitable to integrate the stiff system of ordinary differential SIRV equations.

Acknowledgments

FH acknowledges the support of the Conselho Nacional de Desenvolvimento Científico e Tecnológico (CNPq).

Data availability statement

All data that support the findings of this study are included within the article (and any supplementary files).

ORCID iDs

F Haas https://orcid.org/0000-0001-8480-6877
M Kröger https://orcid.org/0000-0003-1402-6714
R Schlickeiser https://orcid.org/0000-0003-3171-5079

References

[1] Kermack W O and McKendrick A G 1927 A contribution to the mathematical theory of epidemics *Proc. R. Soc.* A **115** 700
[2] Kendall D G 1956 Deterministic and stochastic epidemics in closed populations *Proc. 3rd Berkeley Symp. Math. Statist. and Prob.* vol 4 (Berkeley, United States: Univ. of Calif. Press) pp 149–66
[3] Hethcode H W 2000 The mathematics of infectious diseases *SIAM Rev.* **42** 599–653
[4] Keeling M J and Rohani F 2008 *Modeling Infectious Diseases in Humans and Animals* (Princeton, NJ: Princeton University Press)
[5] Estrada E 2020 Covid-19 and SARS-CoV-2. Modeling the present, looking at the future *Phys. Rep.* **869** 1
[6] Kröger M and Schlickeiser R 2021 Verification of the accuracy of the SIR model in forecasting based on the improved SIR model with a constant ratio of recovery to infection rate by comparing with monitored second wave data *R. Soc. Open Sci.* **8** 211379
[7] Heng K and Althaus C L 2020 The approximately universal shapes of epidemic curves in the susceptible–exposed–infectious–recovered (SEIR) model *Sci. Rep.* **10** 19365
[8] Liu J, Peng B and Zhang T 2015 Effect of discretization on dynamical behavior of SEIR and SIR models with nonlinear incidence *Appl. Math. Lett.* **39** 60–6
[9] Bailey N T J 1975 *The Mathematical Theory of Infectious Diseases and its Applications* 2nd edn (London: Griffin)
[10] Assadouq A, El Mahjour H and Settati A 2020 Qualitative behavior of a SIRS epidemic model with vaccination on heterogeneous networks *Ital. J. Pure Appl. Math.* **43** 958–74
[11] Elbasha E H, Podder C N and Gumel A B 2011 Analyzing the dynamics of an SIRS vaccination model with waning natural and vaccine-induced immunity *Nonlinear Anal.: Real World Appl.* **12** 2692–705
[12] Gakkhar S and Negi K 2008 Pulse vaccination in SIRS epidemic model with non-monotonic incidence rate *Chaos Solitons Fractals* **35** 626–38
[13] Schlickeiser R and Kröger M 2021 Analytical modeling of the temporal evolution of epidemics outbreaks accounting for vaccinations *Physics* **3** 386

[14] Holm D D, Marsden J E, Ratiu T and Weinstein A 1985 Nonlinear stability of fluid and plasma equilibria *Phys. Rep.* **123** 2–116
[15] Badin G and Barry A M 2018 Collapse of generalized Euler and surface quasigeostrophic point vortices *Phys. Rev.* E **98** 023110
[16] Bloch A M and Marsden J E 1990 Stabilization of rigid body dynamics by the energy-Casimir method *Syst. Control Lett.* **14** 341–6
[17] García I A and Hernández-Bermejo B 2017 Inverse Jacobi multiplier as a link between conservative systems and Poisson structures *J. Phys. A: Math. Theor.* **50** 325204
[18] Nutku Y 1990 Bi-Hamiltonian structure of the Kermack–Mckendrick model for epidemics *J. Phys. A: Math. Gen.* **23** L1145–6
[19] Gümral H and Nutku Y 1993 Poisson structure of dynamical systems with three degrees of freedom *J. Math. Phys.* **34** 5691
[20] Haas F and Goedert J 1994 On the generalized Hamiltonian structure of 3D dynamical systems *Phys. Lett.* A **199** 173
[21] Goedert J, Haas F, Hua D, Feix M R and Cairó L 1994 Generalized Hamiltonian structures for systems in three dimensions with a rescalable constant of motion *J. Phys. A: Math. Gen.* **27** 6495–507
[22] Ballesteros A, Blasco A and Gutierrez-Sagredo I 2020 Hamiltonian structure of compartmental epidemiological models *Physica* D **413** 132656
[23] Hernández-Bermejo B 2006 New four-dimensional solutions of the Jacobi equations for Poisson structures *J. Math. Phys.* **47** 022901
[24] Esen O, Choudhury A G, Guha P and Gümral H 2016 Superintegrable cases of four-dimensional dynamical systems *Regul. Chaot. Dyn.* **21** 175–88
[25] Haas F 2002 Generalized Hamiltonian structures for Ermakov systems *J. Phys. A: Math. Gen.* **35** 2925–35
[26] Marciniak K and Rauch-Wojciechowski S 1998 Two families of nonstandard Poisson structures for Newton equations *J. Math. Phys.* **39** 5292–306
[27] Littlejohn R G 1979 A guiding center Hamiltonian: a new approach *J. Math. Phys.* **20** 2445
[28] Littlejohn R G 1982 Hamiltonian perturbation theory in noncanonical coordinates *J. Math. Phys.* **23** 742
[29] Cary J R and Littlejohn R G 1983 Noncanonical Hamiltonian mechanics and its application to magnetic field line flow *Ann. Phys., NY* **151** 1
[30] Hernández-Bermejo B and Fairén V 1998 Hamiltonian structure and Darboux theorem for families of generalized Lotka–Volterra systems *J. Math. Phys.* **39** 6162
[31] Plank M 1995 Hamiltonian structures for then-dimensional Lotka–Volterra equations *J. Math. Phys.* **36** 3520–34
[32] Hernández-Bermejo B and Fairén V 2000 Separation of variables in the Jacobi identities *Phys. Lett.* A **271** 258–63
[33] Bhaskara K H and Rama K 1991 Quadratic Poisson structures *J. Math. Phys.* **32** 2319–22
[34] Liu Z-J and Xu P 1992 On quadratic Poisson structures *Lett. Math. Phys.* **26** 33
[35] Schlickeiser R and Kröger M 2021 Analytical solution of the SIR-model for the temporal evolution of epidemics: B. Semi-time case *J. Phys. A: Math. Theor.* **54** 175601
[36] Kröger M and Schlickeiser R 2020 Analytical solution of the SIR-model for the temporal evolution of epidemics: A: Time-independent reproduction factor *J. Phys. A: Math. Theor.* **53** 505601
[37] Abramowitz M and Stegun I (ed) 1965 *Handbook of Mathematical Functions with Formulas, Graphs and Mathematical Tables* (New York: Dover)
[38] Weisstein E 2009 *The CRC Encyclopedia of Mathematics* 3rd edn (London: Chapman and Hall)
[39] Shankar P M 2021 *Differential Equations: A Problem Solving Approach Based on MATLAB* (Boca Raton, FL: CRC Press)
[40] Beyer W H 1987 *CRC Standard Mathematical Tables* 28th edn (Boca Raton, FL: CRC Press) p 455
[41] Nambu Y 1973 Generalized Hamiltonian dynamics *Phys. Rev.* D **7** 2405
[42] Shishanin A O 2018 Nambu mechanics and its applications *IOP Conf. Ser.: Mater. Sci. Eng.* **468** 012029
[43] Müller A and Névir P 2014 A geometric application of Nambu mechanics: the motion of three point vortices in the plane *J. Phys. A: Math. Theor.* **47** 105201
[44] Evans N W 1990 Superintegrability in classical mechanics *Phys. Rev.* A **41** 5666